

SUPPLEMENTARY MATERIAL TO

Chemical reactivity of alliin and its molecular interactions with the M protease^{pro} of SARS-CoV-2

WENDOLYNE LÓPEZ-OROZCO, LUIS HUMBERTO MENDOZA-HUIZAR*, GIAAN ARTURO ÁLVAREZ-ROMERO, JESÚS MARTÍN TORRES-VALENCIA, AND MARICRUZ SANCHEZ-ZAVALA

Academic Area of Chemistry, Universidad Autónoma del Estado de Hidalgo, Carretera Pachuca-Tulancingo, 42184, Mineral de la Reforma, Hidalgo, Mexico

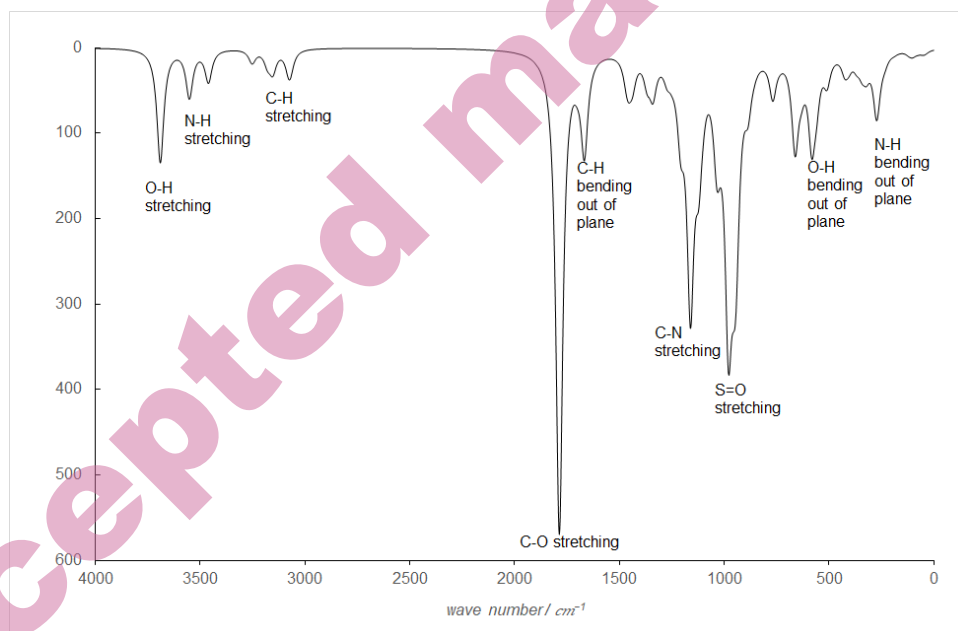


Figure S-1: Theoretical IR spectra of alliin in the aqueous phase obtained at the B3LYP/DGDZVP level of theory.

* Corresponding author E-mail: hhuizar@uaeh.edu.mx

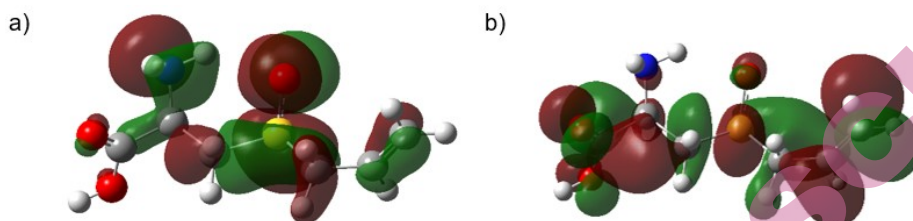


Figure S-2. HOMO and LUMO distributions on alliin obtained at the B3LYP/DGDZVP level of theory in the gas phase. In all cases the isosurfaces were obtained at 0.08 e/u.a.^3 .

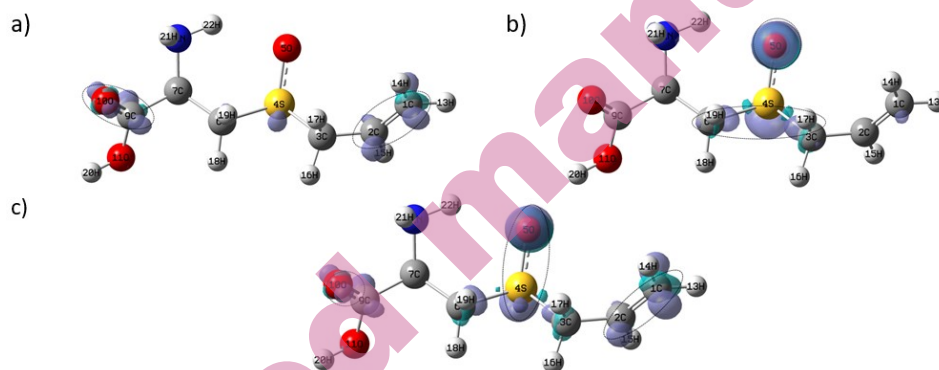


Figure S-3. Isosurfaces of Fukui Functions for alliin according to equations (9), (10) and (11) at the B3LYP/DGDZVP level of theory in the gas phase. In the case of (a) nucleophilic, (b) electrophilic and (c) free radical attacks. In all cases the isosurfaces were obtained at 0.008 e/u.a.^3 . The dotted circles show the most reactive zones in each molecule.

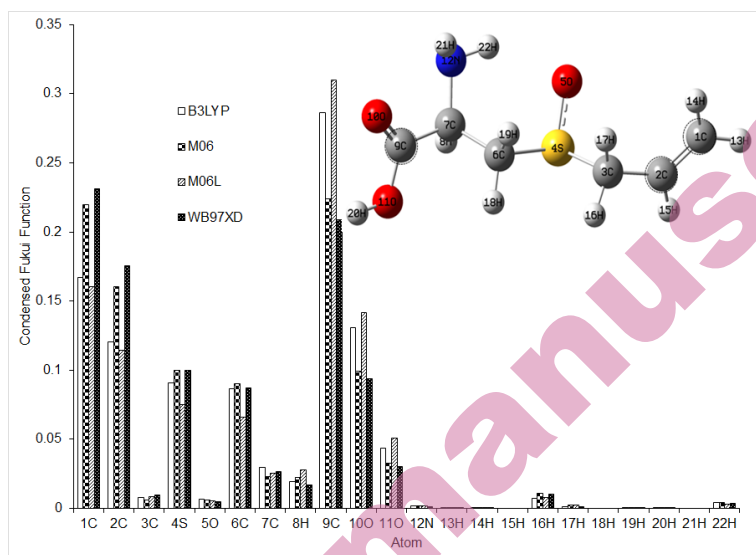


Figure S-4. Condensed Fukui function values for electrophilic attacks on alliin at the X/DGDZVP level of theory (where X=B3LYP, M06, M06L and ω B97XD), in the aqueous phase employing the Hirshfeld population and equations (12)-(14), the dashed circles show the most reactive zones in each molecule.

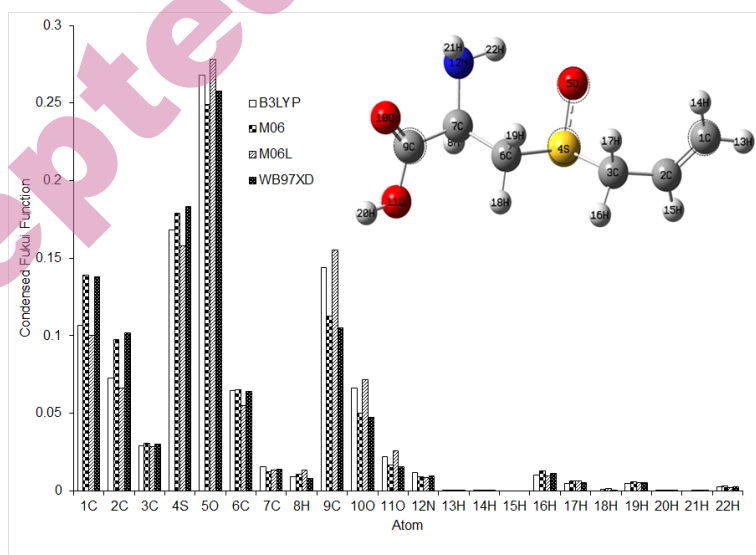


Figure S-5. Condensed Fukui function values for free radical attacks on alliin at the X/DGDZVP level of theory (where X=B3LYP, M06, M06L and ω B97XD), in the aqueous phase employing the Hirshfeld population and equations (12)-(14), the dashed circles show the most reactive zones in each molecule.

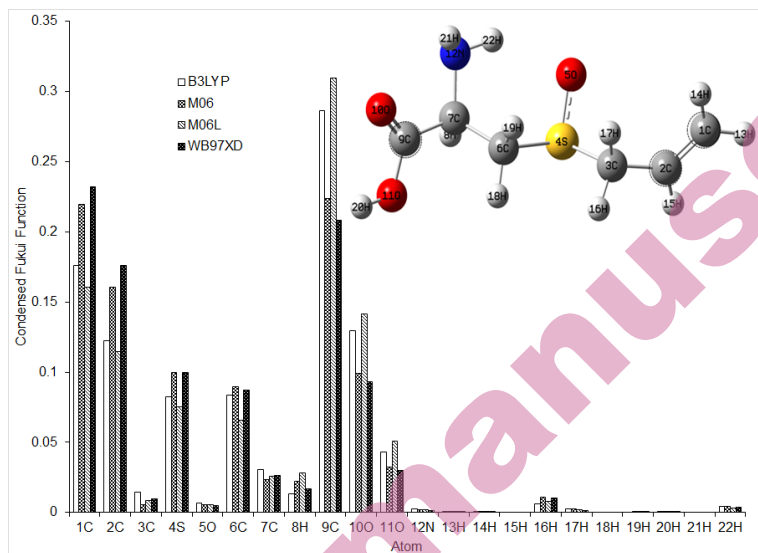


Figure S-6. Condensed Fukui function values for nucleophilic attacks on alliin at the X/DGDZVP level of theory (where X=B3LYP, M06, M06L and ω B97XD), in the gas phase employing the Hirshfeld population and equations (12)-(14), the dashed circles show the most reactive zones in each molecule.

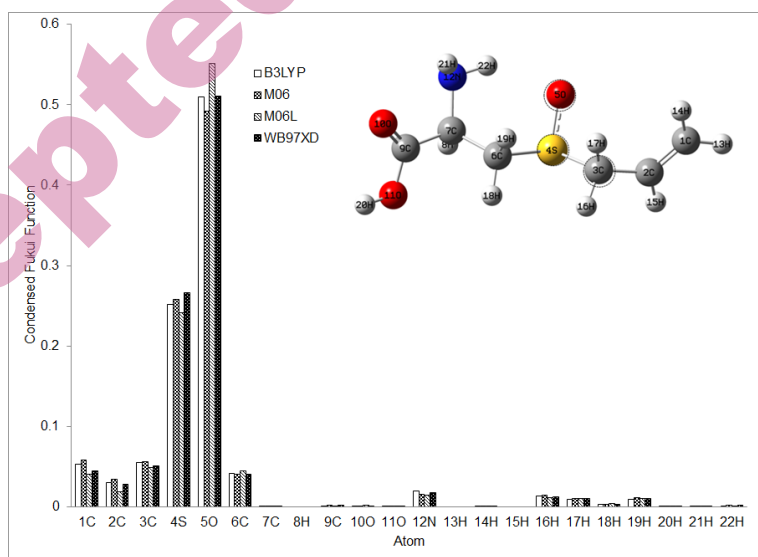


Figure S-7. Condensed Fukui function values for electrophilic attacks on alliin at the X/DGDZVP level of theory (where X=B3LYP, M06, M06L and ω B97XD), in the gas phase employing the Hirshfeld population and equations (12)-(14), the dashed circles show the most reactive zones in each molecule.

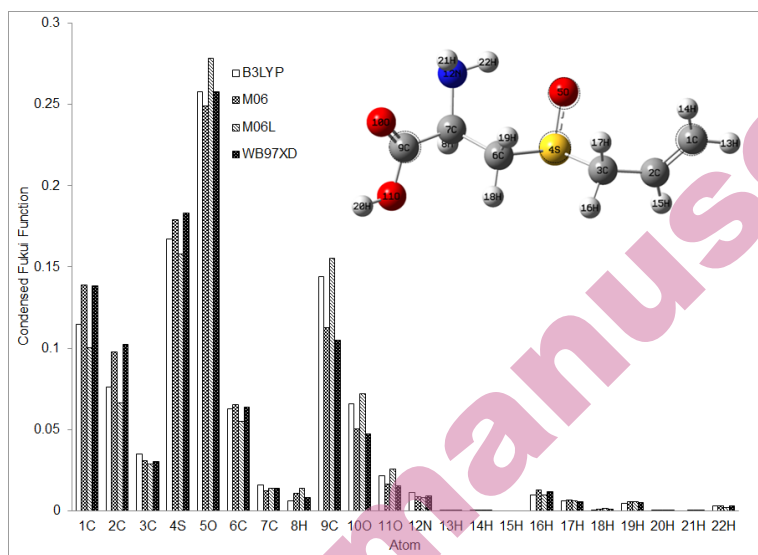


Figure S-8. Condensed Fukui function values for free radical attacks on alliin at the X/DGDZVP level of theory (where X=B3LYP, M06, M06L and ωB97XD), in the gas phase employing the Hirshfeld population and equations (12)-(14), the dashed circles show the most reactive zones in each molecule.

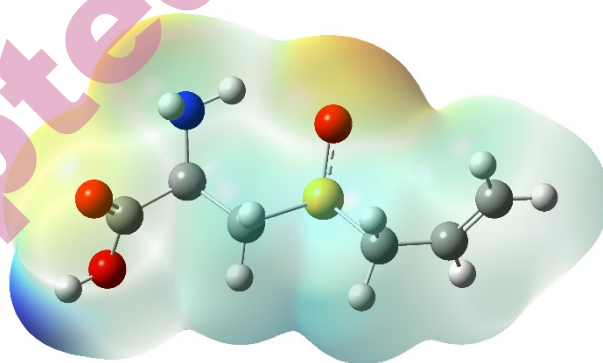


Figure S-9. Mapping of electrostatic potentials evaluated at the B3LYP/DGDZVP level of theory in the gas phase, over a density isosurface (value = 0.002 e/a.u.³) for alliin.

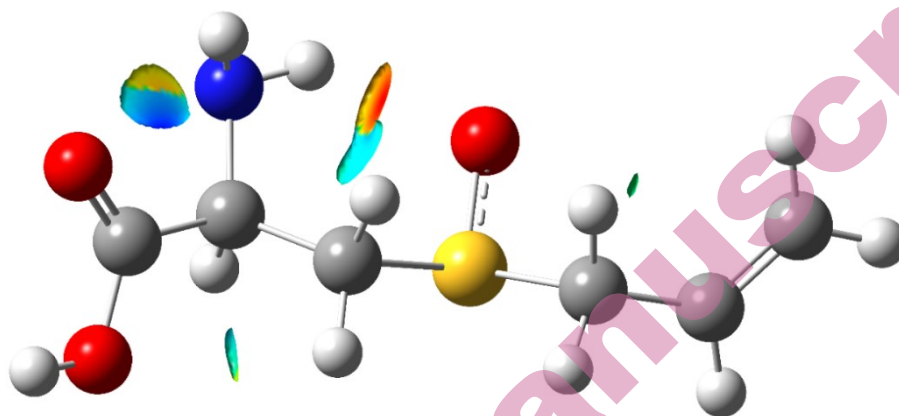
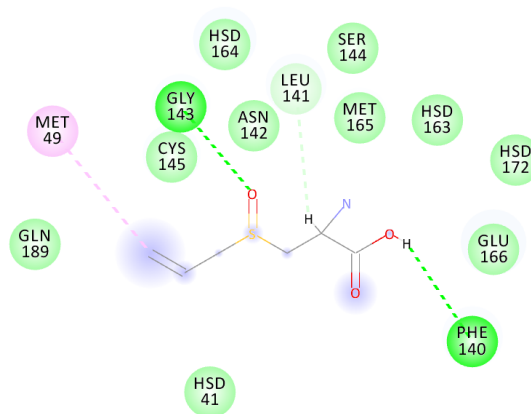


Figure S-10. Isosurface area of $\text{NCI} = 0.2$ for alliin in aqueous phase.



Interactions
van der Waals
Conventional Hydrogen Bond

Carbon Hydrogen Bond
Alkyl

Figure S-11. 2D mapping of ligand/protein interactions for alliin.